# Fingers Crossed: Optical Activity of a Chiral Dimer of Plasmonic Nanorods

Baptiste Auguié,*[,†] José Lorenzo Alonso-Gómez,[‡] Andrés Guerrero-Martínez,[†] and Luis M. Liz-Marzán*[,†]

[†]Departamento de Química Física and [‡]Departamento de Química Orgánica, Universidade de Vigo, Spain

**ABSTRACT:** We investigate theoretically the optical activity of a dimer of plasmonic nanoantennas, mimicking the geometry of a molecule with two isolated chromophores, a situation commonly described as exciton coupling in organic chemistry. As the scale of the system increases and approaches the wavelength of visible light, a rich variety of effects arise that are unique to the plasmonic case. Scattering of light by the particles, negligible in very small clusters, strongly perturbs, and eventually dominates, the optical activity. Additionally, retardation effects in dimers with an interparticle separation commensurate with the wavelength of the incident light affect the electromagnetic coupling between the particles and lead to an asymmetric circular dichroism spectrum. We identify conditions for efficient interaction and predict remarkably large anisotropy factors.



**SECTION:** Nanoparticles and Nanostructures
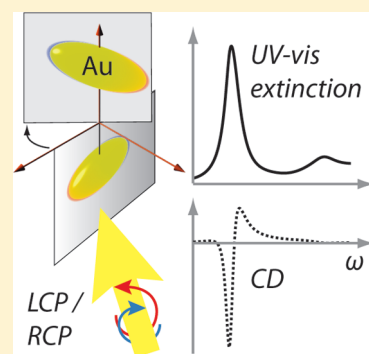
Optical activity from plasmonic nanoparticles is a rapidly emerging field at the frontier of nanophotonics and conventional spectroscopy.[1,2] This interest stems from the multidisciplinary nature of possible applications in biology,[3] chemistry,[4,5] and optics of novel metamaterials.[6,7] The pursuit of plasmonic optical activity is justified by the potential cooperation between two key components. First, studies of optical activity, circular dichroism (CD) in particular, in a chiral sample can reveal a wealth of detailed structural information.[4,8] Second, plasmonic nanoparticles confer the host material unique and exquisitely tunable optical properties in the UV–vis–near-IR range.[9–12] Nanoparticles of coinage metals can act as nanoantennas for visible light, whereby the electromagnetic field undergoes a resonant interaction with the conduction electrons of the particle, known as localized surface plasmon resonance (LSPR).[13,14] The optical cross section characterizing the strength of the interaction between the sample and incident light in scattering and absorption can be enhanced several fold with respect to the physical area of the particle.[10,15] The excitation of LSPRs is also accompanied by focusing of the electromagnetic field in subwavelength mode volumes near the particle boundary,[16,17] a property that finds many applications in surface-enhanced spectroscopies.[18] A direct consequence of these electromagnetic properties is the strong sensitivity of plasmonic nanoantennas to their immediate environment and, in particular, the interaction between adjacent particles[19] that leads to a hybridization of the LSPR modes supported by the individual particles.[20–29] In the context of optical activity, the precise arrangement of nanoparticles in a chiral structure is crucial.[5,30] Theoretical studies, as well as initial experimental demonstrations, have shown the potential of gold nanoparticles, nanorods in particular, to produce surface-plasmon-mediated CD (SP-CD) signals of outstanding intensity.[30–33]

While the theoretical description of circular dichroism in a wide variety of molecular systems is a mature field with a long history,[34] the consideration of nanometer-sized metallic particles introduces many new challenges. A variety of numerical methods are used in the plasmonics literature to investigate the optical properties of metal nanoparticles; these methods are principally based on classical electrodynamics of continuous media,[25,35] in contrast to the first-principle calculations achievable in molecular systems or metal clusters with a more modest number of atoms.[36] In this context, the present work aims at providing new insight into some of the physical phenomena associated with CD in three-dimensional chiral plasmonic nanostructures. Using a coupled dipole model not unlike exciton coupling theory,[23] we investigate the influence of the geometrical parameters of a chiral dimer of gold nanorods on its CD response. Our model extends the recent contribution of Govorov and co-workers[30] by considering anisotropic particles, which have been shown to provide a higher potential for SP-CD.[31] Further, we consider the finite size of the particles and study its effect on the optical activity of the dimer through the concomitant contributions of scattering and retardation.

*Exciton Coupling in a Dimer of Gold Nanorods.* Figure 1a illustrates the system under consideration, a dimer of gold nanorods represented as prolate ellipsoids in a homogeneous surrounding medium of refractive index $n = 1.5$ (typical value for glass). Ellipsoidal particles, while not used in most experiments (nanorods, in particular, are closer in shape to spherically capped cylinders), offer a convenient prototype for a wider class of nonspherical particles using analytical formulas for their polarizability. In this work, we follow the polarizability prescription of
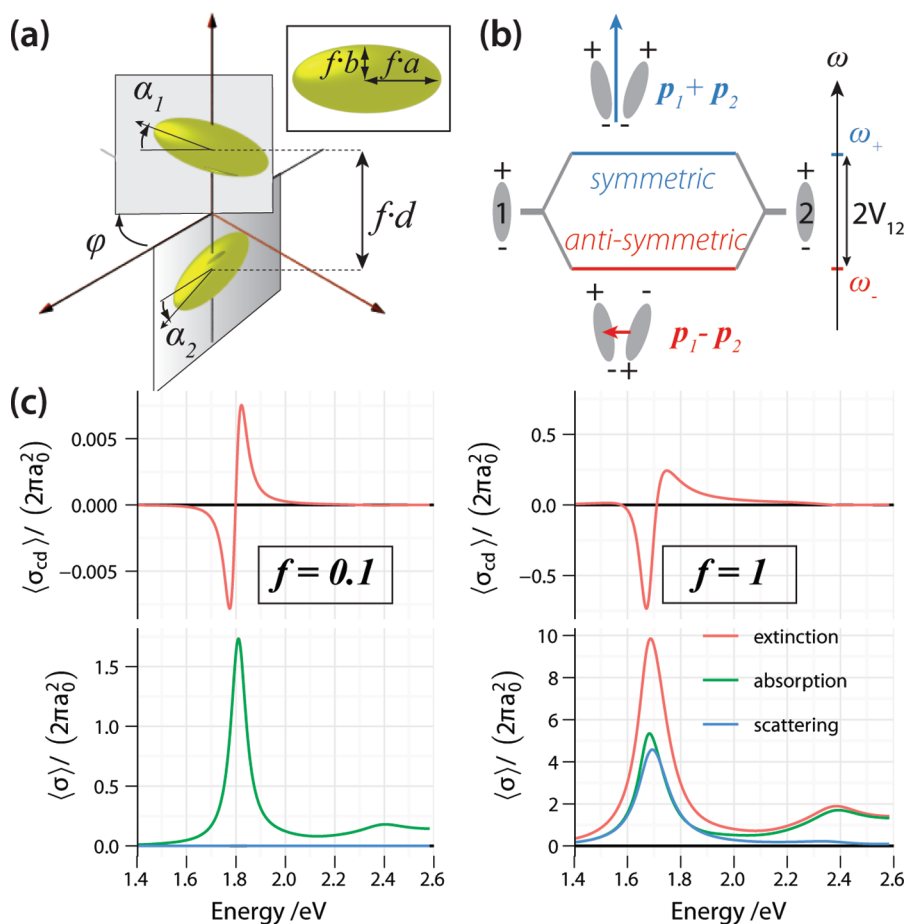
**Figure 1.** (a) Schematic representation of a dimer of gold nanorods with interparticle separation $f \cdot d$ taken from center-to-center and the relative orientation specified by $\varphi = 10°$ (dihedral angle), $\alpha_1 = 10°$, and $\alpha_2 = 20°$. Each particle is represented as a prolate ellipsoid with semiaxes $f \cdot a$ and $f \cdot b$. (b) Energy diagram of the LSPR hybridization of two identical dipoles $\mathbf{p}_1$ and $\mathbf{p}_2$. The electromagnetic interaction splits the two degenerate LSPR modes into a symmetric mode with higher energy $\omega_+$ and an antisymmetric mode with lower energy $\omega_-$. For a dimer of nanorods to be chiral, the two dipoles cannot be exactly parallel; therefore, the antisymmetric mode is not totally "dark" (nonzero dipole moment). (c) Coupled dipole calculations of the extinction, absorption, and scattering efficiency and CD efficiency for the dimer represented in (a), with a scaling factor of $f = 0.1$ (left, $f \cdot a = 4$ nm, $f \cdot b = 1.5$ nm, $f \cdot d = 10$ nm) and $f = 1$ (right, $f \cdot a = 40$ nm, $f \cdot b = 15$ nm, $f \cdot d = 100$ nm). The efficiency is defined as the optical cross section normalized by twice the geometrical cross section of a sphere with equivalent volume to that of the ellipsoid.

Kuwata et al., which has proven accurate for subwavelength particles of moderate aspect ratio.[37] The radiative damping correction included in this prescription is essential to correctly describe the scattering cross section of the particles.

Ignoring for the moment the contribution of the transverse LSPR modes, the system can be idealized to a dimer of two dipoles $\mathbf{p}_1$ and $\mathbf{p}_2$ oriented along the long axis of each ellipsoid. This is precisely the situation considered in exciton coupling theory, which we now describe qualitatively to provide some physical insight into the dipole–dipole interaction mechanism.[8]

Light incident on the dimer causes each dipole to radiate an electromagnetic field, which in turn affects its neighboring dipole. This dipole–dipole interaction is associated with an energy[8,23,38]

$$V_{12} = \frac{p_1 p_2}{n R_{12}^3}(\hat{\mathbf{e}}_1 \cdot \hat{\mathbf{e}}_2 - 3(\hat{\mathbf{e}}_1 \cdot \hat{\mathbf{e}}_{12})(\hat{\mathbf{e}}_2 \cdot \hat{\mathbf{e}}_{12})) \qquad (1)$$

(in the quasi-static limit) separating the new energy levels corresponding to the symmetric ($\omega_+$) and antisymmetric ($\omega_-$) hybrid modes to the energy level of the LSPR (Figure 1b). Here $\hat{\mathbf{e}}_{1,2} = \mathbf{p}_{1,2}/\|\mathbf{p}_{1,2}\|$, $\mathbf{r}_{12}$ is the vector joining the two dipoles, and $\hat{\mathbf{e}}_{12} = \mathbf{r}_{12}/\|\mathbf{r}_{12}\|$. The resulting CD spectrum can be obtained by summing

the extinction band associated with each hybrid mode, with a strength and sign described by a rotational strength $R = \mathrm{Im}(\mathbf{p} \cdot \mathbf{m})$, where $\mathbf{p}$ and $\mathbf{m}$ stand for the electric and magnetic dipole moments, respectively. In the situation of two interacting electric dipoles, this expression reduces to[8]

$$R^{\pm} = \pm \frac{\pi}{2\lambda_0} \mathbf{r}_{12} \cdot (\mathbf{p}_1 \times \mathbf{p}_2) \qquad (2)$$

$\lambda_0$ being the wavelength of the uncoupled LSPR. $R^{\pm}$ changes sign between the symmetric and antisymmetric hybrid modes, which results in a characteristic bisignated line shape for the CD spectrum (a positive band followed by a negative band or vice versa). The sign of $R^{\pm}$ for a given mode is dictated by the dihedral angle $\varphi$, which makes a natural parametrization of the dimer. The rotational strength would appear to be optimized when $\mathbf{r}_{12} \parallel (\mathbf{p}_1 \times \mathbf{p}_2)$; however, $\mathbf{p}_1 \perp \mathbf{p}_2$ yields a zero CD signal as the dimer is achiral, and the two hybrid modes are degenerate ($V_{12} = 0$). The geometry that yielded the most intense CD in our numerical simulations (all based on the more accurate coupled dipole approximation,[30,31] including retardation) was obtained for $\varphi = \pi/4$, $\alpha_1 = \alpha_2 = 0$.

Shown in Figure 1c are the results of the coupled dipole modeling of two such dimers with a different scale. The coupled dipole equations and their application to circular dichroism calculations have been described in several previous works.[30,31] On the left-hand side, we illustrate the situation most closely approaching the molecular system described by exciton coupling theory while resting on the realm of continuous electrodynamics, with a scaling factor of $f = 0.1$. The scattering, absorption, and extinction cross sections are averaged over all possible incident angles and normalized by the effective area corresponding to twice the geometrical cross section of an equivolume sphere of radius $a_0 = (ab^2)^{1/3}$. For such small particles, extinction is largely dominated by absorption, which peaks at the LSPR associated with the long axis ($\sim$1.8 eV) and short axis ($\sim$2.4 eV) of the ellipsoids. The CD spectrum, corresponding to the difference in extinction for light of left-handed and right-handed circular polarization, shows an antisymmetrical line shape centered about the longitudinal LSPR mode, with much smaller intensity than the extinction ($\sigma_{cd}/\sigma_{ext} \approx 0.01$). On the right-hand side, we show the result for $f = 1$, a dimer of gold nanoparticles with dimensions typical of state-of-the-art colloidal synthesis. The spectral line shape is similar to the previous case; the spectral position of the longitudinal LSPR is not strongly affected by the particle volume at a constant particle aspect ratio for subwavelength particles. Upon closer inspection, however, important differences are noticeable. First, scattering and absorption contribute to the same extent to the overall extinction associated with the longitudinal LSPR. Second, the (adimensional) maximum extinction efficiency has increased by a factor of $\sim$6 upon scaling of the system.

The ratio of CD over extinction has also increased by a factor of $\sim$8, illustrating the potential of plasmonic nanoparticles to produce intense optical activity. The CD line shape remains conservative (null integrated area); however, the shape departs from the antisymmetric curve predicted by exciton coupling theory. The high-energy wing is weaker and broader than its low-energy counterpart.

*Radiative Reaction and Retardation Effects.* We now set out to explain these new features unique to the larger-scale plasmonic system by investigating how the finite size of the sample (compared to the wavelength) affects its optical properties.

Presented in Figure 2 are the simulated spectra in the coupled dipole approximation with and without retardation in the dipolar field. The coupled dipole approximation initiated by DeVoe,[39] as well as its application in exciton coupling theory,[8] considered only the quasi-static term of the dipolar field responsible for the electromagnetic coupling between dipoles. When the interparticle distance approaches a fraction of the wavelength, however, retardation effects start to play an important role as the phase of the electromagnetic field coupling the two dipoles varies with the distance; we find that these retardation effects are largely responsible for the asymmetry in the CD line shape. Another effect that participates in the asymmetry of the CD spectrum is the coupling between the longitudinal and transverse modes; however, this effect is relatively minor here because of the considerable energy and intensity differences between the two resonances.

We illustrate in Figure 3 the influence of the scattering contribution to the circular dichroism. The dimer corresponds to that shown in Figure 1a with parameters $\varphi = \pi/4$ and $\alpha_1 = \alpha_2 = 0$. The particle size is scaled by a factor of $s$, while the interparticle distance is kept constant ($d = 100$ nm).
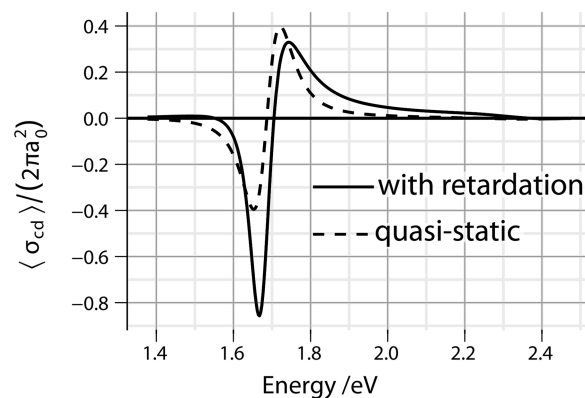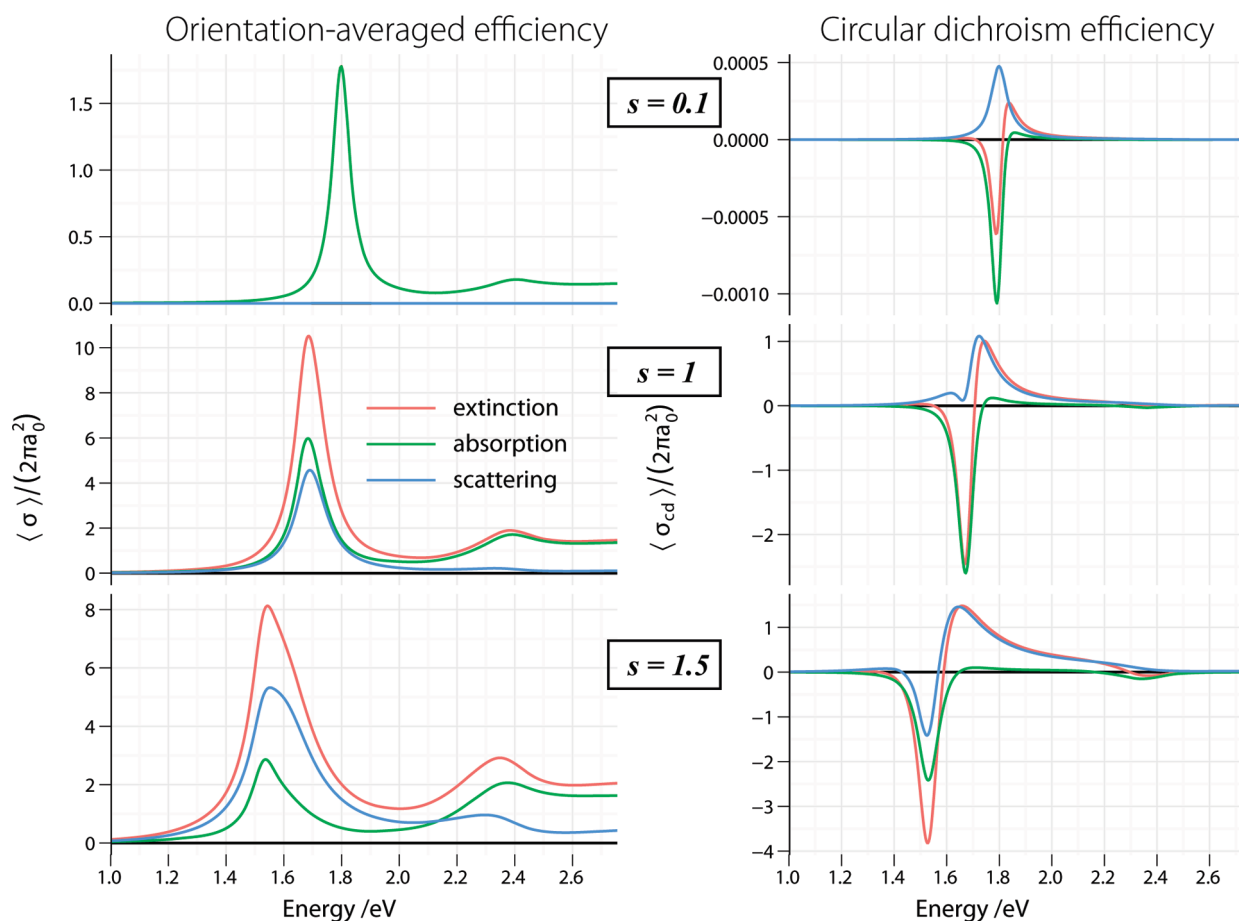


**Figure 2.** Coupled dipole simulations of the CD spectrum for a dimer of gold nanorods with parameters $f = 1$, $d = 100$ nm, $\varphi = \pi/4$, $\alpha_1 = \alpha_2 = 0$, $a = 40$ nm, and $b = 15$ nm. For the dashed curve, the expression for the electromagnetic field coupling the two dipoles is truncated to the static term, while the solid curve considers the full dipolar coupling, including retardation.

For $s < 0.1$, the extinction and absorption efficiencies nearly coincide, and the associated CD signal presents an asymmetric line shape centered at the longitudinal LSPR energy. Interestingly, while scattering is very weak, its contribution to the CD signal is on par with that of absorption and is monosigned (only a positive band here). The absorption contribution to the CD is nonconservative (unequal positive and negative integrated spectral bands) and weaker on the high-energy side. The overall CD signal (extinction) is conservative with zero integrated area, in accordance with a general sum rule for circular dichroism;[40] however, it presents a shape asymmetry that is due to retardation (weaker and broader tail on the high-energy side).

In the hybridization picture, the nearly dark mode depicted in Figure 1b originates from an antibonding combination of the two longitudinal LSPRs, with the highest electric field density situated at the location of the particles.[29] Thus, the field distribution should be more concentrated inside of the particles, where the ohmic losses occur, for the dark mode than for the bright mode. This is reflected in the nearly monosigned absorption contribution to the CD spectrum. Conversely, the bright mode has a large net electric dipole moment, and as a consequence, we should expect more radiative loss for the bright mode, which results in a monosigned scattering contribution to the CD spectrum.

When the particle length approaches $\sim$80 nm ($s = 1$ here), scattering and absorption contribute equally to the extinction of the dimer. This is also the regime where the absorption cross section of the dipolar mode is maximized,[41] as well as the absorption and extinction efficiencies. The absorption contribution to the CD is still strongly asymmetric, with only the low-energy band subsisting. The scattering contribution compensates to ensure the conservative overall CD (extinction), with a broader high-energy wing. A small low-energy feature appears in the scattering contribution.

As the scale of the dimer increases further ($s \approx 1.5$), scattering dominates over absorption and dictates the extinction spectrum at the longitudinal LSPR energy. The ratio of CD over extinction also increases; the next section will be devoted to a discussion of this effect. The transverse plasmon band, pinned near the region of interband transitions in gold, starts to gain intensity through radiative damping. Correspondingly, a small CD feature appears at this energy, with a mixing between transverse and longitudinal

## Orientation-averaged efficiency

## Circular dichroism efficiency



**Figure 3.** (Left) Coupled dipole simulations of the scattering, absorption, and extinction efficiency spectra for a dimer of gold nanorods with increasing particle size, $s \cdot a \times s \cdot b$ ($a = 40$ nm, $b = 15$ nm), with fixed separation $d = 100$ nm. (Right) Corresponding CD efficiencies. The angles parametrizing the dimer are $\varphi = \pi/4$ and $\alpha_1 = \alpha_2 = 0$.
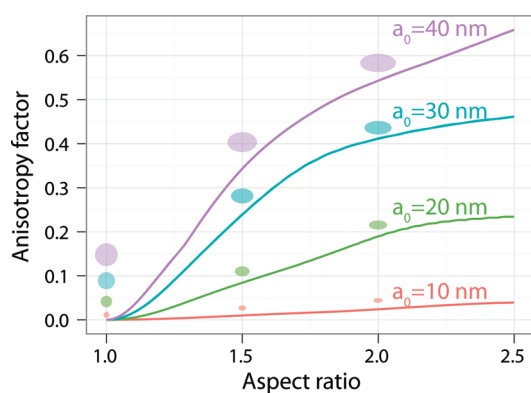


**Figure 4.** Coupled dipole simulations of the peak value of the anisotropy factor $g = 2(|\sigma_L - \sigma_R|)/(\sigma_L + \sigma_R)$ for a dimer of gold nanorods with parameters $d = 100$ nm, $\varphi = \pi/4$, and $\alpha_1 = \alpha_2 = 0$. The particle size is varied with aspect ratio ranging from 1:1 (sphere) to 2.5:1 (prolate ellipsoid). The particle volume is indicated as the radius $a_0 = (ab^2)^{1/3}$ of an equivolume sphere. Scaled outlines of the different ellipsoidal shapes are shown in different colors.

CD bands. The CD band of the longitudinal LSPR is dominated by the scattering contribution, which forms a slightly asymmetric bisignated band with a skew toward the high-energy side.

*Influence of the Particle Aspect Ratio.* The extinction efficiency predicted in Figure 3 to be much greater than unity for an optimum scale of the dimer illustrates the capacity of plasmonic nanoantennas to focus light into subwavelength regions of space; with a suitable aspect ratio, a gold nanorod can interact with the incident electromagnetic field with an effective area tens of times larger than its projectional area (geometrical optics), as illustrated by Bohren and Huffman.[10] This remarkable property of subwavelength particles of noble metals stems from the capacity of their nearly free conduction electrons to react to and screen an incident electromagnetic field. The strong oscillator strength characterizing their response is compressed into a narrow spectral region of LSPR excitation by reducing the particle size to a subwavelength domain of bulk material. Changing the shape and aspect ratio of the particle with a constant volume (number of free charges) affects the position and spectral width of the LSPR; from this, we can understand how the aspect ratio plays an important role in determining the strength of the light—particle interaction. To conclude this study, we evaluate the influence of the aspect ratio of the nanoparticles in the strength of the CD signal.

In Figure 4, results are shown for the evolution of the anisotropy factor $g = 2(\sigma_L - \sigma_R)/(\sigma_L + \sigma_R)$, characterizing the relative strength of CD over extinction and often used as a measure of optical activity,[4] as a function of particle volume and aspect ratio $a/b$. A dimer of nanospheres is achiral; in fact, four

spheres are required to form a chiral system.[30,31] Correspondingly, the maximum g-factor vanishes for small aspect ratios, irrespective of the particle volume. As the aspect ratio increases, the anisotropy factor rapidly rises with a sigmoid-like trend. We note that the CD efficiency of a chiral dimer of nanorods is a nonlinear function of the aspect ratio of the particles, as well as their volume. The interplay between absorption and scattering, discussed in Figure 3, is apparent in the different trend between small and larger particle volumes. The maximum g-factor appears to be for the larger particle size (where scattering dominates), at least within the domain of validity of the coupled dipole approximation used in this work. It is expected that the influence of higher-order multipolar contributions will substantially affect the CD response at higher particle volumes and aspect ratios or shorter interparticle separation. Additionally, cooperative effects between more than two gold nanorods have been shown to augment the CD signal.[31]

These promising numerical results should stimulate the experimental investigation of colloidal metal nanoparticles as a new approach to obtain strong optical activity with plasmonic metamaterials. Top-down lithography techniques have recently enabled the fabrication of a variety of chiral metamaterials;[42−45] however, the proposed structures have often been two-dimensional and periodic, which limits their range of application in terms of angle of incidence and frequency. It is also difficult to manufacture arrays of subwavelength particles with good resolution and a unit cell smaller than the working wavelength in the visible regime. In contrast, chiral dimers of nanorods could be obtained via chemical synthesis in solution using a chiral binding agent between nanorods, thereby forming a truly three-dimensional, homogeneous, and isotropic chiral metamaterial.

Beyond the well-studied mechanism of exciton coupling in molecular systems, we have identified a number of peculiar features in the plasmonic counterpart. First, as the size parameter, that is, the product of the linear dimension of the scatterer times the wavevector, approaches unity, the strength of the CD increases dramatically.[30] Second, the aspect ratio of the nanoparticles is predicted to be an essential parameter in producing intense optical activity, in agreement with a recent experimental study where the use of nonspherical particles proved instrumental in measuring a CD response.[31]

Conversely, the physical insight of exciton coupling theory highlights a few notable features of the CD spectrum of a chiral dimer of plasmonic nanoantennas. The bisignated line shape stems from the contribution of two hybrid modes of the structure. It is worth noting that although one of the bands originates from the antibonding mode, which would be a dark mode if the dipoles were exactly parallel, its integrated intensity is equal to that of the bonding mode. CD spectroscopy thus offers a novel way to probe a nearly dark mode in a plasmonic structure and perhaps to benefit from its low radiative losses.

## ■ AUTHOR INFORMATION

### Corresponding Author
*E-mail: baptiste.auguie@uvigo.es (B.A.); lmarzan@uvigo.es (L.M.L.-M.).

## ■ ACKNOWLEDGMENT

## ■ REFERENCES

(1) Gautier, C.; Bürgi, T. Chiral Gold Nanoparticles. ChemPhysChem 2009, 10, 483–492.

(2) Noguez, C.; Garzón, I. L. Optically Active Metal Nanoparticles. Chem. Soc. Rev. 2009, 38, 757–771.

(3) Amabilino, D. B., Ed. Chirality at the Nanoscale; Wiley-VCH: New York, 2008.

(4) Berova, N.; Bari, L. D.; Pescitelli, G. Application of Electronic Circular Dichroism in Configurational and Conformational Analysis of Organic Compounds. Chem. Soc. Rev. 2007, 36, 914.

(5) Chen, W.; Bian, A.; Agarwal, A.; Liu, L.; Shen, H.; Wang, L.; Xu, C.; Kotov, N. A. Nanoparticle Superstructures Made by Polymerase Chain Reaction: Collective Interactions of Nanoparticles and a New Principle for Chiral Materials. Nano Lett. 2009, 9, 2153–2159.

(6) Pendry, J. B. A Chiral Route to Negative Refraction. Science 2004, 306, 1353–1355.

(7) Gubler, U.; Bosshard, C. Optical Materials: A New Twist for Nonlinear Optics. Nat. Nanotechnol. 2002, 1, 209–210.

(8) Harada, N.; Nakanishi, K. Circular Dichroic Spectroscopy: Exciton Coupling in Organic Stereochemistry; University Science Books: Mill Valley, CA, 1983.

(9) Maier, S. A. Plasmonics: Fundamentals and Applications; Springer: New York, 2007.

(10) Bohren, C.; Huffman, D. Absorption and Scattering of Light by Small Particles; Wiley: New York, 1998.

(11) Huang, X.; Neretina, S.; El-Sayed, M. A. Gold Nanorods: From Synthesis and Properties to Biological and Biomedical Applications. Adv. Mater. 2009, 21, 4880–4910.

(12) Grzelczak, M.; Pérez-Juste, J.; Mulvaney, P.; Liz-Marzán, L. Shape Control in Gold Nanoparticle Synthesis. Chem. Soc. Rev. 2008, 37, 1783–1791.

(13) Raether, H. Surface Plasmons on Smooth and Rough Surfaces and on Gratings; Springer: New York, 1988.

(14) Kreibig, U.; Vollmer, M. Optical Properties of Metal Clusters; Springer: Berlin, Germany, 1995.

(15) Bohren, C.; Huffman, D. Absorption Cross-Section Maxima and Minima in IR Absorption-Bands of Small Ionic Ellipsoidal Particles. Appl. Opt. 1981, 20, 959–962.

(16) Alvarez-Puebla, R.; Liz-Marzán, L. M.; García de Abajo, F. J. Light Concentration at the Nanometer Scale. J. Phys. Chem. Lett. 2010, 1, 2428–2434.

(17) Nabika, H.; Takase, M.; Nagasawa, F.; Murakoshi, K. Toward Plasmon-Induced Photoexcitation of Molecules. J. Phys. Chem. Lett. 2010, 1, 2470–2487.

(18) Maier, S. Plasmonic Field Enhancement and SERS in the Effective Mode Volume Picture. Opt. Express 2006, 14, 1957–1964.

(19) Funston, A.; Novo, C.; Davis, T.; Mulvaney, P. Plasmon Coupling of Gold Nanorods at Short Distances and in Different Geometries. Nano Lett. 2009, 9, 1651–1658.

(20) Schmeits, M.; Dambly, L. Fast-Electron Scattering by Bispherical Surface-Plasmon Modes. Phys. Rev. B 1975, 44, 12706–12712.

(21) Prodan, E.; Radloff, C.; Halas, N. J.; Nordlander, P. A Hybridization Model for the Plasmon Response of Complex Nanostructures. Science 2003, 302, 419–422.

(22) Nordlander, P.; Oubre, C.; Prodan, E.; Li, K.; Stockman, M. I. Plasmon Hybridization in Nanoparticle Dimers. Nano Lett. 2004, 4, 899–903.

(23) Jain, P.; Eustis, S.; El-Sayed, M. Plasmon Coupling in Nanorod Assemblies: Optical Absorption, Discrete Dipole Approximation Simulation, and Exciton-Coupling Model. J. Phys. Chem. B 2006, 110, 18243–18253.

850

dx.doi.org/10.1021/jz200279x |J. Phys. Chem. Lett. 2011, 2, 846–851

(24) Jain, P. K.; Huang, W.; El-Sayed, M. A. On the Universal Scaling Behavior of the Distance Decay of Plasmon Coupling in Metal Nanoparticle Pairs: A Plasmon Ruler Equation. *Nano Lett.* **2007**, *7*, 2080–2088.

(25) Myroshnychenko, V.; Rodriguez-Fernandez, J.; Pastoriza-Santos, I.; Funston, A. M.; Novo, C.; Mulvaney, P.; Liz-Marzán, L. M.; García de Abajo, F. J. Modelling the Optical Response of Gold Nanoparticles. *Chem. Soc. Rev.* **2008**, *37*, 1792–1805.

(26) Pramod, P.; Thomas, K. Plasmon Coupling in Dimers of Au Nanorods. *Adv. Mater.* **2008**, *20*, 4300–4305.

(27) Jain, P.; El-Sayed, M. Plasmonic Coupling in Noble Metal Nanostructures. *Chem. Phys. Lett.* **2010**, *487*, 153–164.

(28) Slaughter, L. S.; Wu, Y.; Willingham, B. A.; Nordlander, P.; Link, S. Effects of Symmetry Breaking and Conductive Contact on the Plasmon Coupling in Gold Nanorod Dimers. *ACS Nano* **2010**, *4*, 4657–4666.

(29) Shao, L.; Woo, K. C.; Chen, H.; Jin, Z.; Wang, J.; Lin, H.-Q. Angle- and Energy-Resolved Plasmon Coupling in Gold Nanorod Dimers. *ACS Nano* **2010**, *4*, 3053–3062.

(30) Fan, Z.; Govorov, A. O. Plasmonic Circular Dichroism of Chiral Metal Nanoparticle Assemblies. *Nano Lett.* **2010**, *10*, 2580–2587.

(31) Guerrero-Martínez, A.; Auguié, B.; Alonso-Gómez, J. L.; Gómez-Graña, S.; Džolic, Z.; Žinic, M.; Cid, M. M.; Liz-Marzán, L. M. Intense Optical Activity via 3D Chiral Ordering of Plasmonic Nanoantennas. *Angew. Chem., Int. Ed.* **2011**, DOI: 10.1002/anie.201007536.

(32) Oh, H. S.; Liu, S.; Jee, H.; Baev, A.; Swihart, M. T.; Prasad, P. N. Chiral Poly(fluorene-alt-benzothiadiazole) (PFBT) and Nanocomposites with Gold Nanoparticles: Plasmonically and Structurally Enhanced Chirality. *J. Am. Chem. Soc.* **2010**, *132*, 17346–17348.

(33) George, J.; Thomas, K. G. Surface Plasmon Coupled Circular Dichroism of Au Nanoparticles on Peptide Nanotubes. *J. Am. Chem. Soc.* **2010**, *132*, 2502–2503.

(34) Born, M. On the Theory of Optical Activity. I. General Theory of a System of Coupled Isotropic Oscillators. II. Molecules with a Binary Axis of Symmetry. *Proc. R. Soc. London, Ser. A* **1935**, *150*, 84–105.

(35) Schatz, G. C.; Jensen, L.; Kelly, K. L.; Lazarides, A. A. Electrodynamics of Noble Metal Nanoparticles and Nanoparticle Clusters. *J. Cluster Sci.* **1999**, *10*, 295–317.

(36) Schatz, G. Using Theory and Computation to Model Nanoscale Properties. *Proc. Natl. Acad. Sci. U.S.A.* **2007**, *104*, 6885–6892.

(37) Kuwata, H.; Tamaru, H.; Esumi, K.; Miyano, K. Resonant Light Scattering from Metal Nanoparticles: Practical Analysis beyond Rayleigh Approximation. *Appl. Phys. Lett.* **2003**, *83*, 4625–4627.

(38) Tabor, C.; Haute, D.; El-Sayed, M. Effect of Orientation on Plasmonic Coupling between Gold Nanorods. *ACS Nano* **2009**, *3*, 3670–3678.

(39) DeVoe, H. Optical Properties of Molecular Aggregates. II. Classical Theory of the Refraction, Absorption, and Optical Activity of Solutions and Crystals. *J. Chem. Phys.* **1965**, *43*, 3199–3208.

(40) Smith, D. Superconvergence and Sum Rules for the Optical Constants: Natural and Magneto-Optical Activity. *Phys. Rev. B* **1976**, *13*, 12.

(41) Equalling absorption and scattering rates for the dipole corresponds to a situation of critical coupling.[46]

(42) Plum, E.; Fedotov, V. A.; Schwanecke, A. S.; Zheludev, N. I.; Chen, Y. Giant Optical Gyrotropy Due to Electromagnetic Coupling. *Appl. Phys. Lett.* **2007**, *90*, 223113.

(43) Gansel, J. K.; Thiel, M.; Rill, M. S.; Decker, M.; Bade, K.; Saile, V.; von Freymann, G.; Linden, S.; Wegener, M. Gold Helix Photonic Metamaterial as Broadband Circular Polarizer. *Science* **2009**, *325*, 1513–5.

(44) Wang, B.; Zhou, J.; Koschny, T.; Kafesaki, M.; Soukoulis, C. M. Chiral Metamaterials: Simulations and Experiments. *J. Opt. A: Pure Appl. Opt.* **2009**, *11*, 114003.

(45) Zhang, S.; Park, Y.-S.; Li, J.; Lu, X.; Zhang, W.; Zhang, X. Negative Refractive Index in Chiral Metamaterials. *Phys. Rev. Lett.* **2009**, *102*, 023901.

(46) Bliokh, K.; Freilikher, V.; Savel'ev, S.; Nori, F. Colloquium: Unusual Resonators: Plasmonics, Metamaterials, and Random Media. *Rev. Mod. Phys.* **2008**, *80*, 1201–1213.